AIAA JOURNAL
Vol. 38, No. 6, June 2000

Use of Substructural Transmission Zeros for Structural Health Monitoring

Gregory W. Reich* and K. C. Park†
University of Colorado, Boulder, Colorado 80309

A method of localized structural health monitoring is presented that utilizes an invariance property of transmission zeros of substructural frequency response functions. These functions are obtained by partitioning the global dynamic flexibility into a substructural form. It is shown that the transmission zeros of the frequency response functions of a damaged substructure are invariant whereas those of healthy substructures are affected. The present method exploits this invariance property for the detection of damage in a structure. Numerical examples are presented to demonstrate the utility of the proposed method.

Introduction

THE increased use of aircraft in service beyond their original life expectancy, together with the aging of today's civil infrastructure, has pushed the discipline of structural health monitoring to the forefront of structures technology. Critical issues such as crack detection, growth models, and mitigation are being addressed, as are structural integrity determination, nondestructive testing and evaluation, and on-site inspections. Research in these areas has been driven by the solution of inverse problems. The particular inverse problem in structural health monitoring, which this paper investigates, is the determination of damage location in a structure.

Methods that have been utilized for identifying the onset, location, and level of damage in a structure can be categorized as non-model based or model based. Non-model-based damage detection takes a signal processing approach[1,2] that makes no correlation to a physical model, whereas model-based analysis is closely tied to a reference finite element or other representative mathematical model of the structure. Of the two, model-based methods have been the most widely adopted. A comprehensive review of this body of literature has recently been compiled.[3]

The prevailing model-based damage detection methods can be further broken down into methods that utilize a global model vs those that utilize a local model. In the global approach the analysis is tied to a global reference model, and the damage is determined at a global location on the structure. In the local approach the model is decomposed into substructures, and therefore, the damage location is determined in terms of substructural quantities. It has been shown[4–7] that the use of substructural system flexibility properties can significantly enhance the prediction of damage location and mechanisms as well as damage levels.

A typical frequency response function (FRF) can be characterized by its zeros and poles (characteristic roots of the numerator and denominator of the FRF). Note that damage impacts both the poles and zeros. Properties of the system poles have been extensively investigated for damage detection purposes, whereas properties of the system transmission zeros have been predominantly ignored. Afolabi[8] appears to be the first to investigate the properties of transmission zeros of global receptance functions for damage detection in simple spring–mass systems. The current method expands on this work to develop a damage detection system that utilizes the zeros of substructural transfer functions.

This paper addresses the determination of the damage location in a structure with an associated reference model. There are two key ideas in the proposed method. The first is the application of a flexibility partitioning theory[9,10] to transform the system dynamics into a localized form. The second is the identification of the transmission zeros of partitions of the localized system transfer functions corresponding to individual substructures. We will show that these particular transmission zeros remain invariant to stiffness changes occurring in that substructure, thereby enabling us to determine the location of damage in the structure.

Properties of Global Transmission Zeros

The discrete linear equations of motion for a structure with typical sensors and actuators for vibration testing can be expressed as

$$\boldsymbol{M}_g\ddot{\boldsymbol{u}}_g + \boldsymbol{C}_g\dot{\boldsymbol{u}}_g + \boldsymbol{K}_g\boldsymbol{u}_g = \mathcal{B}_g\boldsymbol{f}_g, \qquad \boldsymbol{y}_g = \mathcal{C}_0\boldsymbol{u} + \mathcal{C}_1\dot{\boldsymbol{u}} + \mathcal{C}_2\ddot{\boldsymbol{u}} \tag{1}$$

where $\boldsymbol{u}_g$ is the displacement vector of the assembled structure; $\boldsymbol{M}_g$, $\boldsymbol{C}_g$, and $\boldsymbol{K}_g$ are the assembled mass, damping, and stiffness matrices; $\boldsymbol{f}_g$ is the applied force; $\mathcal{B}_g$ is the excitation location operator; $\mathcal{C}_{(0,1,2)}$ are the sensor placement Boolean matrices; $\boldsymbol{y}_g$ is the measurement output vector; $(\dot{})$ denotes time differentiation; and the subscript g refers to the global structural system, as opposed to the partitioned substructures that will be introduced later.

In the Laplace domain, with $\dot{\boldsymbol{u}}(0) = \boldsymbol{u}(0) = 0$ and $\mathcal{C}_g = \mathcal{C}_0$, Eq. (1) can be rewritten to solve for the output as

$$\tilde{\boldsymbol{y}}_g(s) = \mathcal{H}_g(s)\tilde{\boldsymbol{f}}_g(s)$$

$$\mathcal{H}_g(s) = \mathcal{C}_g\left(\boldsymbol{K}_g + s\boldsymbol{C}_g + s^2\boldsymbol{M}_g\right)^{-1}\mathcal{B}_g = \mathcal{C}_g\bar{\mathcal{K}}_g^{-1}(s)\mathcal{B}_g \tag{2}$$

where

$$\bar{\mathcal{K}}_g(s) = \left(\boldsymbol{K}_g + s\boldsymbol{C}_g + s^2\boldsymbol{M}_g\right) \tag{3}$$

is defined as the global dynamic stiffness matrix, and

$$[\tilde{\boldsymbol{y}}_g(s),\ \tilde{\boldsymbol{f}}_g(s)] = \int_0^\infty [\boldsymbol{y}_g(t),\ \boldsymbol{f}_g(t)]e^{-st}\,\mathrm{d}t \tag{4}$$

are the Laplace transformed output and input, respectively.

In a typical vibration test setting it is neither practical to excite all of the modes nor to place sensors sufficient to cover every discrete degree of freedom (DOF) desired. Nevertheless, for the clarity of our discussion, we will assume that the entire displacement vector is measured and that $\mathcal{B}_g$ is an identity matrix whose size is the same as $\boldsymbol{u}_g$. Note that a matrix element $h_{g_{i,j}}$ of $\mathcal{H}_g$ can be expressed[11] in terms of the cofactor of $\bar{\mathcal{K}}_g$,

$$h_{g_{i,j}} = \frac{\operatorname{cof}\bar{\mathcal{K}}_g(i,\ j)}{\det\bar{\mathcal{K}}_g} \tag{5}$$

where

$$\operatorname{cof}\bar{\mathcal{K}}_g(i,\ j) = (-1)^{i+j}\det\bar{\mathcal{K}}_g^{j,i} \tag{6}$$

Received 14 July 1999; revision received 22 November 1999; accepted for publication 3 December 1999.

*U.S. Air Force Palace Knight Graduate Research Fellow, Campus Box 429, Center for Aerospace Structures; reich@titan.colorado.edu. Member AIAA.

†Professor, Aerospace Engineering, Campus Box 429, Center for Aerospace Structures; kcpark@titan.colorado.edu.

The submatrix $\bar{K}_g^{j,i}$ is obtained by deleting row j and column i from $\bar{K}_g$. Thus, the poles of $\mathcal{H}_g$ and the zeros of an element $h_{g_{i,j}}$ are given by

$$\text{poles of } \mathcal{H}_g \Rightarrow \text{the roots of } \det \bar{K}_g = 0$$

$$\text{zeros of } h_{g_{i,j}} \Rightarrow \text{the roots of cof} \bar{K}_g(i, j) = 0 \tag{7}$$

A generalization of this statement is that the transmission zeros of a block partition of $\mathcal{H}_g$ corresponding to DOF lists $(\mathcal{L}, m)$ are computed by finding the roots of $\text{cof} \bar{K}_g(\mathcal{L}, m) = 0$, which is found from the determinant of the submatrix of $\bar{K}_g$ without rows m and columns $\mathcal{L}$.

Note that the transmission zeros of a multi-input/multi-output (MIMO) transfer function $\mathcal{H}_g(s)$ that satisfies $\tilde{y}_g(s) = \mathcal{H}_g(s)\tilde{f}_g(s)$ do not correspond in general to the zeros of an individual scalar element $h_{g_{i,j}}(s)$ of the transfer function matrix $\mathcal{H}_g(s)$. However, if the transfer function has only a single input and a single output, then the transfer function is a scalar function, and the transmission zeros of that transfer function are indeed equal to the antiresonances of the scalar function.

Observe that, due to the definition of the matrix cofactor, changes in the stiffness and/or mass properties at node n do not affect the zeros of the block partition $\mathcal{H}_g(n, n)$. It is this node-by-node invariance property of the global system zeros that was exploited by Afolabi[8] in his attempt to detect damage. The node-by-node zero invariance property, however, does not accurately predict damage for general structures, except for elements at a fixed boundary. First, structural failures occur in arbitrary locations and very rarely coincide with an isolated node. Second, for continuum and trusslike structures, a nodal stiffness is made up of contributions from the elements that are connected to that node.

The preceding observations have motivated us to develop a damage detection method based on an element-by-element transmission zero invariance property. To this end, we offer a review of the structural partitioning procedure that forms the basis both for inverse algorithms and for the partitioned solution of structural problems on parallel computers.

Dynamic Substructural Flexibility Theory

In this section, we will show how the global transfer functions are transformed into a form based on the strain (or deformation) present in each substructure. This formulation reveals the relation between the global equations of motion and the partitioned equations of motion. In other words, one relates the global FRF $\mathcal{H}_g(\omega)$ to that of strain-based partitioned structures.

Linear Equations of Motion

We begin with the global form of the energy functional of a discrete structural system:

$$\Pi(\boldsymbol{u}_g) = \boldsymbol{u}_g^T\left(\tfrac{1}{2}\boldsymbol{K}_g\boldsymbol{u}_g + \boldsymbol{C}_g\dot{\boldsymbol{u}}_g + \boldsymbol{M}_g\ddot{\boldsymbol{u}}_g - \boldsymbol{f}_g\right) \tag{8}$$

As a reminder, the global equations of motion are determined from this equation by finding the stationary value of the energy functional $\delta\Pi = 0$:

$$\boldsymbol{M}_g\ddot{\boldsymbol{u}}_g + \boldsymbol{C}_g\dot{\boldsymbol{u}}_g + \boldsymbol{K}_g\boldsymbol{u}_g = \boldsymbol{f}_g \tag{9}$$

The unique global FRF can then be determined by transforming the preceding equation into the frequency domain and solving for $\hat{\boldsymbol{u}}_g$:

$$\hat{\boldsymbol{u}}_g = \mathcal{H}_g(\omega)\hat{\boldsymbol{f}}_g, \qquad \mathcal{H}_g(\omega) = \left(\boldsymbol{K}_g + j\omega\boldsymbol{C}_g - \omega^2\boldsymbol{M}_g\right)^{-1}$$

$$\begin{Bmatrix}\hat{\boldsymbol{u}}_g \\ \hat{\boldsymbol{f}}_g\end{Bmatrix} = e^{j\omega t}\begin{Bmatrix}\boldsymbol{u}_g \\ \boldsymbol{f}_g\end{Bmatrix} \tag{10}$$

where the terms indicated with a caret denote frequency-domain representations of the variable. Note that this equation is the equivalent of the Laplace domain transfer function in Eq. (2) given the substitution $s = j\omega$. In this paper, the terms transfer function and FRF will be used interchangeably, with the understanding that they are not technically synonymous.

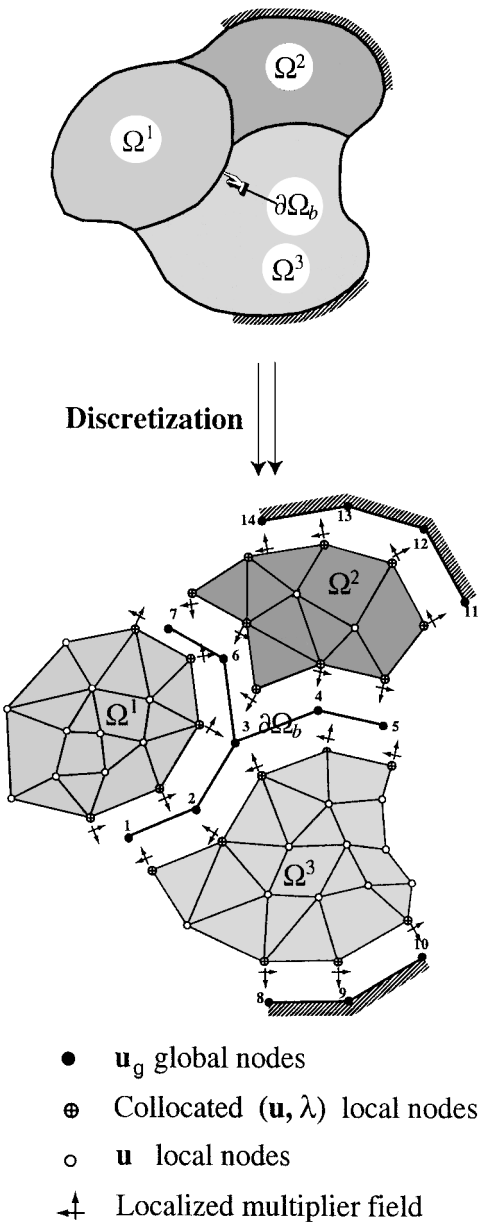

Fig. 1 Structural partitioning process.

Partitioning

Consider the structure shown in Fig. 1. From top to bottom, Fig. 1 represents the disassembly or partitioning process of the global structure into its substructural parts. On the top, a generic continuum structure is shown, complete with natural boundary conditions and an underlying pattern of subdomains. On the bottom, the structure is shown after the partitioning and discretization process is complete. Each subdomain is represented by internal and boundary nodes (local nodes), as well as the interface forces or multiplier field that relate each local node to the corresponding global node. Note that, after partitioning, the global nodes that lie on the partition boundaries are co-owned by two or more substructures. Partitioning is the disassembly process given by

$$\boldsymbol{u} = \boldsymbol{L}\boldsymbol{u}_g \tag{11}$$

where $\boldsymbol{u}$ is the vector of substructural displacements and $\boldsymbol{L}$ is the Boolean disassembly matrix that relates the global and substructural displacements. The elemental force vector that is conjugate to $\boldsymbol{u}$ is given as

$$\boldsymbol{L}^T\boldsymbol{f} = \boldsymbol{f}_g \tag{12}$$

In addition, the global stiffness matrix $\boldsymbol{K}_g$ is formed by the assembly of individual substructural stiffnesses via the operator $\boldsymbol{L}$:

$$\boldsymbol{K}_g = \boldsymbol{L}^T \boldsymbol{K} \boldsymbol{L}, \qquad \boldsymbol{K} = \begin{bmatrix} \boldsymbol{K}^{(1)} & & & & \\ & \boldsymbol{K}^{(1)} & & & \\ & & \boldsymbol{K}^{(s)} & & \\ & & & \ddots & \\ & & & & \boldsymbol{K}^{(n_s)} \end{bmatrix} \tag{13}$$

where $\boldsymbol{K}$ is the block-diagonal collection of unassembled substructural stiffness matrices $\boldsymbol{K}^{(s)}$.

To maintain the kinematic compatibility of the global and local displacements, the substructural displacements must satisfy the following:

$$\boldsymbol{B}_\lambda (\boldsymbol{u} - \boldsymbol{L}\boldsymbol{u}_g) = 0 \tag{14}$$

where a generic constraint matrix $\boldsymbol{B}_\lambda$ is introduced. This constraint matrix can be chosen in one of several ways. It can be a Boolean matrix that extracts the boundary nodes of partitioned substructures or it can be chosen as a nullspace of the disassembly operator $\boldsymbol{L}$:

$$\boldsymbol{B}_\lambda^T \boldsymbol{L} = 0 \tag{15}$$

Using Eqs. (11–14), the energy functional of Eq. (8) can be rewritten in terms of the substructural displacement and constraints as

$$\Pi(\boldsymbol{u}, \boldsymbol{\lambda}, \boldsymbol{u}_g) = \boldsymbol{u}^T \left(\tfrac{1}{2}\boldsymbol{K}\boldsymbol{u} + \boldsymbol{C}\dot{\boldsymbol{u}} + \boldsymbol{M}\ddot{\boldsymbol{u}} - \boldsymbol{f} \right) + \boldsymbol{\lambda}^T \boldsymbol{B}_\lambda^T (\boldsymbol{u} - \boldsymbol{L}\boldsymbol{u}_g) \tag{16}$$

where $\boldsymbol{M}$ and $\boldsymbol{C}$ are the substructural mass and damping matrices, respectively. A vector of Lagrange multipliers $\boldsymbol{\lambda}$ that enforces the kinetic compatibility constraint must also be introduced. These variables can be thought of as the interface forces created between substructures by the partitioning process.

Derivation of Strain-to-Displacement Relation

A fundamental problem in determining strain-based FRFs is the expression of displacement in terms of strain, rather than the converse. Note that the displacement $\boldsymbol{u}$ of a free–free partitioned substructure can be decomposed[9] into a deformation $\boldsymbol{d}$ and a rigid-body motion $\boldsymbol{r}$:

$$\boldsymbol{u} = \boldsymbol{d} + \boldsymbol{r} = \boldsymbol{d} + \boldsymbol{\Phi}_\alpha \boldsymbol{\alpha} \tag{17}$$

In the second term, the rigid-body motion is decomposed into $\boldsymbol{\Phi}_\alpha$, which describes the rigid-body modes of the element and is only dependent on the element geometry and type, and $\boldsymbol{\alpha}$, which represent the associated generalized coordinates.

The strain–displacement relationship for discrete elements can be written as

$$\boldsymbol{\epsilon} = \boldsymbol{S}\boldsymbol{u} \tag{18}$$

where $\boldsymbol{S}$ can be determined in a variety of ways, for example, from the finite element shape functions of the corresponding discrete elements. This equation can be combined with Eq. (17) and results in the expression of strain in terms of deformation:

$$\boldsymbol{\epsilon} = \boldsymbol{S}(\boldsymbol{d} + \boldsymbol{\Phi}_\alpha \boldsymbol{\alpha}) = \boldsymbol{S}\boldsymbol{d} \tag{19}$$

because the rigid-body modes $\boldsymbol{\Phi}_\alpha$ do not incur any strain. The inverse of this equation results in an equation for the elemental deformation in terms of the elemental strain:

$$\boldsymbol{d} = \boldsymbol{\Phi}_\epsilon \boldsymbol{\epsilon}, \qquad \boldsymbol{\Phi}_\epsilon = \boldsymbol{S}^+ \tag{20}$$

Combining this equation with Eq. (17) results in the desired relation, that is, expressing the elemental displacements in terms of the elemental strain and rigid-body motion:

$$\boldsymbol{u} = \boldsymbol{\Phi}_\epsilon \boldsymbol{\epsilon} + \boldsymbol{\Phi}_\alpha \boldsymbol{\alpha} = \boldsymbol{\Phi} \begin{Bmatrix} \boldsymbol{\epsilon} \\ \boldsymbol{\alpha} \end{Bmatrix} \tag{21}$$

Examples of this formulation for simple elements may be found in the paper by Park and Reich.[7]

Strain-Based Equations of Motion

The strain-to-displacement relationship of Eq. (21) can now be inserted into the energy function in Eq. (16). This results in the energy functional expressed in terms of the elemental strain, rigid-body motion, and the interface forces:

$$\Pi(\boldsymbol{\epsilon}, \boldsymbol{\alpha}, \boldsymbol{\lambda}) = (\boldsymbol{\Phi}_\epsilon \boldsymbol{\epsilon} + \boldsymbol{\Phi}_\alpha \boldsymbol{\alpha})^T \left\{ \tfrac{1}{2}\boldsymbol{K}(\boldsymbol{\Phi}_\epsilon \boldsymbol{\epsilon} + \boldsymbol{\Phi}_\alpha \boldsymbol{\alpha}) + \boldsymbol{C}(\boldsymbol{\Phi}_\epsilon \dot{\boldsymbol{\epsilon}} + \boldsymbol{\Phi}_\alpha \dot{\boldsymbol{\alpha}}) + \boldsymbol{M}(\boldsymbol{\Phi}_\epsilon \ddot{\boldsymbol{\epsilon}} + \boldsymbol{\Phi}_\alpha \ddot{\boldsymbol{\alpha}}) - \boldsymbol{f} \right\} + \boldsymbol{\lambda}^T \boldsymbol{B}_\lambda^T (\boldsymbol{\Phi}_\epsilon \boldsymbol{\epsilon} + \boldsymbol{\Phi}_\alpha \boldsymbol{\alpha}) \tag{22}$$

By choosing $\boldsymbol{B}_\lambda$ as in Eq. (15), the dependence on the global displacement $\boldsymbol{u}_g$ is removed. The stationary value of this functional yields the partitioned, strain-based equations of motion:

$$\begin{bmatrix} \left(\boldsymbol{M}_\epsilon \frac{d^2}{dt^2} + \boldsymbol{C}_\epsilon \frac{d}{dt} + \boldsymbol{K}_\epsilon\right) & \left(\boldsymbol{M}_{\epsilon\alpha} \frac{d^2}{dt^2} + \boldsymbol{C}_{\epsilon\alpha} \frac{d}{dt}\right) & \boldsymbol{\Phi}_\epsilon^T \boldsymbol{B}_\lambda \\ \left(\boldsymbol{M}_{\epsilon\alpha}^T \frac{d^2}{dt^2} + \boldsymbol{C}_{\epsilon\alpha}^T \frac{d}{dt}\right) & \left(\boldsymbol{M}_\alpha \frac{d^2}{dt^2} + \boldsymbol{C}_\alpha \frac{d}{dt}\right) & \boldsymbol{\Phi}_\alpha^T \boldsymbol{B}_\lambda \\ \boldsymbol{B}_\lambda^T \boldsymbol{\Phi}_\epsilon & \boldsymbol{B}_\lambda^T \boldsymbol{\Phi}_\alpha & \boldsymbol{0} \end{bmatrix} \begin{Bmatrix} \boldsymbol{\epsilon} \\ \boldsymbol{\alpha} \\ \boldsymbol{\lambda} \end{Bmatrix} = \begin{Bmatrix} \boldsymbol{\Phi}_\epsilon^T \boldsymbol{f} \\ \boldsymbol{\Phi}_\alpha^T \boldsymbol{f} \\ \boldsymbol{0} \end{Bmatrix} \tag{23}$$

This equation can be simplified by denoting the following:

$$\boldsymbol{\Phi} = [\boldsymbol{\Phi}_\epsilon \quad \boldsymbol{\Phi}_\alpha], \qquad \boldsymbol{K}_\phi = \boldsymbol{\Phi}^T \boldsymbol{K} \boldsymbol{\Phi} = \begin{pmatrix} \boldsymbol{K}_\epsilon & \boldsymbol{0} \\ \boldsymbol{0} & \boldsymbol{0} \end{pmatrix}$$

$$\boldsymbol{M}_\phi = \boldsymbol{\Phi}^T \boldsymbol{M} \boldsymbol{\Phi} = \begin{pmatrix} \boldsymbol{M}_\epsilon & \boldsymbol{M}_{\epsilon\alpha} \\ \boldsymbol{M}_{\epsilon\alpha}^T & \boldsymbol{M}_\alpha \end{pmatrix}, \qquad \boldsymbol{C}_\phi = \boldsymbol{\Phi}^T \boldsymbol{C} \boldsymbol{\Phi} = \begin{pmatrix} \boldsymbol{C}_\epsilon & \boldsymbol{C}_{\epsilon\alpha} \\ \boldsymbol{C}_{\epsilon\alpha}^T & \boldsymbol{C}_\alpha \end{pmatrix}$$

$$\boldsymbol{\phi} = \begin{Bmatrix} \boldsymbol{\epsilon} \\ \boldsymbol{\alpha} \end{Bmatrix}, \qquad \boldsymbol{f}_\phi = \boldsymbol{\Phi}^T \boldsymbol{f} \tag{24}$$

In the frequency domain, this results in

$$\begin{bmatrix} (\boldsymbol{K}_\phi + j\omega \boldsymbol{C}_\phi - \omega^2 \boldsymbol{M}_\phi) & \boldsymbol{B}_\phi \\ \boldsymbol{B}_\phi^T & \boldsymbol{0} \end{bmatrix} \begin{Bmatrix} \hat{\boldsymbol{\phi}} \\ \hat{\boldsymbol{\lambda}} \end{Bmatrix} = \begin{Bmatrix} \hat{\boldsymbol{f}}_\phi \\ \boldsymbol{0} \end{Bmatrix} \tag{25}$$

where $\boldsymbol{B}_\phi = \boldsymbol{\Phi}^T \boldsymbol{B}_\lambda$. The corresponding strain-based FRF can be determined from this equation by eliminating $\hat{\boldsymbol{\lambda}}$:

$$\hat{\boldsymbol{\phi}} = \mathcal{H}_\phi(\omega) \hat{\boldsymbol{f}}_\phi, \qquad \mathcal{H}_\phi(\omega) = \boldsymbol{Z}_\phi - \boldsymbol{Z}_\phi \boldsymbol{B}_\phi \left[\boldsymbol{B}_\phi^T \boldsymbol{Z}_\phi \boldsymbol{B}_\phi\right]^{-1} \boldsymbol{B}_\phi^T \boldsymbol{Z}_\phi$$

$$\boldsymbol{Z}_\phi = \left(\boldsymbol{K}_\phi + j\omega \boldsymbol{C}_\phi - \omega^2 \boldsymbol{M}_\phi\right)^{-1} \tag{26}$$

where $\mathcal{H}_\phi(\omega)$ is designated as the strain-based FRF.

It cannot be emphasized enough that the FRF in Eq. (10) relates the global inputs to the global outputs. That is, the displacements, accelerations, velocities, or force measurements taken from the physical structure are global, and the model derived from that data relates quantities from the assembled structure. In contrast to that is the preceding equation, which describes the relationship between quantities unique to each substructure.

The difference between the global FRF and the localized FRF can be conceptualized as is shown in Fig. 2. The traditional system identification method, shown on the left, measures inputs and outputs from the global system and determines the FRF relating the two. A localized system identification procedure, shown on the right, measures inputs and outputs from the partitioned system. The FRF and other identified characteristics correspond to this partitioned system. As is described in Fig. 2, the interface forces are automatically included when the local outputs are determined.

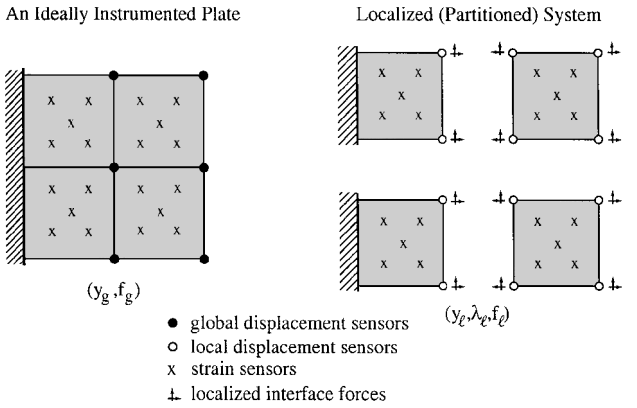

Fig. 2 Comparison between global and local FRFs: global FRFs, $\mathcal{H}_g(\omega) = [\hat{y}_g^*(\omega) \cdot \hat{f}_g(\omega)]/[\hat{f}_g^*(\omega) \cdot \hat{f}_g(\omega)]$; and localized FRFs, $\mathcal{H}_\ell(\omega) = [\hat{y}_\ell^*(\omega) \cdot \hat{f}_\ell(\omega)]/[\hat{f}_\ell^*(\omega) \cdot \hat{f}_\ell(\omega)]$. Note: y_ℓ becomes a function of the interaction force λ_ℓ as shown in Eq. (26).

By recalling Eqs. (21) and (11), the relationship between the substructural variables and the global displacements can be determined in the following way:

$$\phi = \begin{Bmatrix} \epsilon \\ \alpha \end{Bmatrix} = \Phi^{-1} L u_g \tag{27}$$

Additionally, invariance of the external work term of the energy functional gives

$$u_g^T f_g = u^T f = \phi^T f_\phi \Rightarrow f_g = L^T \Phi^{-T} f_\phi \tag{28}$$

This equation can then be used in conjunction with the global FRF expression of Eq. (10):

$$\mathcal{H}_\phi(\omega) = \Phi^{-1} L \mathcal{H}_g(\omega) L^T \Phi^{-T} \tag{29}$$

The transfer functions in Eqs. (23) and (29) are equal because of input–output system invariance. Equation (26) highlights the dependence of the localized FRF on the local dynamics of the partitioned form, whereas Eq. (29) highlights the dependence on the global dynamics.

Finally, we note that from Eq. (23) the dynamics of the system in strain-based form are partitioned into the internal strain energy corresponding to the strain DOF and inertial energy corresponding to the rigid-body motion of the system. In particular, if we are to assume that damage occurs only as a change in the stiffness of the structure, then the only terms of interest are those containing K_ϵ. From the definition of Φ in Eq. (24), we can consider only the partition that corresponds to the strain energy of the substructural partitions:

$$\Phi = [\Phi_\epsilon \quad \Phi_\alpha] = [S^+ \quad \Phi_\alpha], \qquad \Phi^{-1} = \begin{pmatrix} S \\ \Phi_\alpha^+ \end{pmatrix} \tag{30}$$

Therefore, we could also determine the partition of the substructural FRFs corresponding to strain energy as

$$\mathcal{H}_\epsilon(\omega) = S L \mathcal{H}_g(\omega) L^T S^T \tag{31}$$

It is this form of the strain-based FRFs that will be utilized to determine the location of damage. This partitioning allows us to use the transmission zeros in a constructive manner. Because the transmission zeros are dependent on the input and output, we have changed them so that they act in an element-by-element manner that can be used for assessing damages.

Damage Detection Based on Transmission Zeros of Partitioned Flexibility

Let us examine the block-diagonal terms in $\mathcal{H}_\epsilon$ corresponding to a individual element e. From Eq. (5), we note that the global FRFs can be expressed as the inverse of the global dynamic stiffness matrix $\bar{K}_g^{-1}$ as

$$\mathcal{H}_g(\omega) = \frac{Z_g}{\det(\bar{K}_g)}, \qquad Z_g = \begin{bmatrix} z_{g_{1,1}} & z_{g_{1,2}} & z_{g_{1,3}} & \cdots & z_{g_{1,n}} \\ z_{g_{1,2}} & z_{g_{2,2}} & z_{g_{2,3}} & \cdots & z_{g_{2,n}} \\ z_{g_{1,3}} & z_{g_{2,3}} & z_{g_{3,3}} & \cdots & z_{g_{3,n}} \\ \cdot & \cdot & \cdot & \cdots & \cdot \\ \cdot & \cdot & \cdot & \cdots & z_{g_{n,n}} \end{bmatrix}$$

$$z_{g_{i,j}} = \operatorname{cof} \bar{K}_g(i, j) \tag{32}$$

where $\operatorname{cof} \bar{K}_g$ is defined in Eq. (6). Note that the numerator in $\mathcal{H}_g$, given by Z_g, is composed of the global dynamic stiffness attributes whereas the denominator is the same for all of the entries in $\mathcal{H}_g$. In other words, the poles are the same for all of the transfer function matrix elements, whereas the zeros are different. Therefore, the global transfer function matrix $\mathcal{H}_g$ is localized according to

$$\mathcal{H}(\omega) = L \mathcal{H}_g(\omega) L^T = Z/\det(\bar{K}_g), \qquad Z = L Z_g L^T \tag{33}$$

because, by Eqs. (11) and (12),

$$\hat{u} = L \hat{u}_g = L \mathcal{H}_g \hat{f}_g = L \mathcal{H}_g L^T \hat{f} = \mathcal{H} \hat{f} \tag{34}$$

Specifically, a matrix element partition $\mathcal{H}(k, k)$ of $\mathcal{H}$ corresponding to element e can be expressed as

$$\mathcal{H}(k, k) = \frac{Z(k, k)}{\det(\bar{K}_g)}, \qquad Z(k, k) = L(k, \ell)\, Z_g(\ell, m) L(m, k)^T \tag{35}$$

where the matrix indices (ℓ, m) are the nonzero row entries in L of columns k. Note that the poles remain unchanged whereas the zeros are localized due to the localization matrix L, which acts only on the elements $Z_g(\ell, m)$. This is an important point, that the poles of a system are not affected by the partitioning transformation. The poles are determined by the global structure alone, and the form of the input and output have no bearing on them whatsoever.

Whereas this process accomplishes the nodal localization of Z_g, it lacks the specific elemental localization necessary. This can be accomplished by transforming Z into the elemental strain-based form:

$$\mathcal{H}_\epsilon = S \mathcal{H} S^T \Rightarrow Z_\epsilon = S Z S^T$$

$$Z_\epsilon(p, p) = S(p, m) Z(m, q) S(q, p)^T \tag{36}$$

which effectively annihilates the attributes corresponding to the localized elemental diagonal rows and columns p of element e as well. This means that the transmission zeros of $\mathcal{H}_\epsilon(p, p)$ would not contain attributes from element e, except perhaps its mass and damping. This observation can now be exploited for the detection of damage and damage locations as follows:

Suppose the zeros of the block-diagonal entries of the strain-based FRF $\mathcal{H}_\epsilon(\omega)$ corresponding to each element are determined both for a healthy reference model as well as the current system whose damage is to be identified. If one detects significant changes in the transmission zeros of some elements when compared to those of the reference model, then the damaged element is the one whose change in its zeros is the minimum.

Theoretically, the variance in a set of transmission zeros (TZs) from the partition of the localized FRF corresponding to the damaged substructure is exactly zero. In practice, however, this may not be the case, and so a numerical measure must be developed to quantitatively determine the relative variance or invariance of a set of TZs. Because the TZs in a particular set vary over a range of frequencies, the quantitative measure used to determine variance is defined as a cumulative error over the range of TZ determined for the particular problem. The error factor is called the cumulative TZ deviation D_{TZ}. For the jth zero computed for a given transfer function, D_{TZ} is given as

$$D_{\mathrm{TZ}}(j) = \operatorname{mean}\left[\left|\frac{z^d(1:j) - z^n(1:j)}{z^d(1:j)}\right|\right] \tag{37}$$

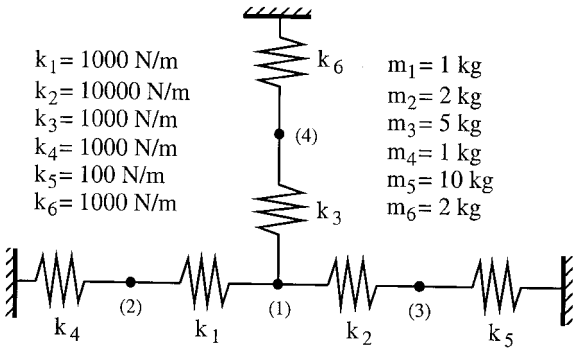

Fig. 3 Spring–mass system.

where z^n indicates the TZ values from a nominal or reference test case and z^d represent those from a follow-up or damaged test case. $\boldsymbol{D}_{\mathrm{TZ}}$ is then a vector for each set of TZs. Each element of the vector is the average variation for each single TZ value up to the current one. $\boldsymbol{D}_{\mathrm{TZ}}$ values are computed separately for each block-diagonal partition of the full transfer function matrix corresponding to separate elements or substructures. The TZ set from the element that has the consistently lowest value of $\boldsymbol{D}_{\mathrm{TZ}}$ over the range of calculated zeros is defined as the element where damage occurs.

To illustrate the present damage identification criterion, consider a spring–mass system as shown in Fig. 3. The global dynamic stiffness of the system can be written as

$$\bar{\boldsymbol{K}}_g = \boldsymbol{K}_g - \omega^2 \boldsymbol{M}_g$$

$$\boldsymbol{K}_g = \begin{bmatrix} k_1 + k_2 + k_3 & -k_1 & -k_2 & -k_3 \\ -k_1 & k_1 + k_4 & 0 & 0 \\ -k_2 & 0 & k_2 + k_5 & 0 \\ -k_3 & 0 & 0 & k_3 + k_6 \end{bmatrix}$$

$$\boldsymbol{M}_g = \begin{bmatrix} \frac{1}{2}(m_1 + m_2 + m_3) & 0 & 0 & 0 \\ 0 & \frac{1}{2}(m_1 + m_4) & 0 & 0 \\ 0 & 0 & \frac{1}{2}(m_2 + m_5) & 0 \\ 0 & 0 & 0 & \frac{1}{2}(m_3 + m_6) \end{bmatrix} \tag{38}$$

where the bar lengths are taken to be unity and the masses are lumped at the two elemental nodes. The product of $\boldsymbol{SL}$ can be expressed as

$$\boldsymbol{SL} = \begin{bmatrix} 1 & -1 & 0 & 0 \\ 1 & 0 & -1 & 0 \\ 1 & 0 & 0 & -1 \\ 0 & 1 & 0 & 0 \\ 0 & 0 & 1 & 0 \\ 0 & 0 & 0 & 1 \end{bmatrix} \tag{39}$$

Carrying out the necessary localization, the matrix element of the strain-based numerator polynomial Z_ϵ corresponding to the first element is given by

$$z_{\epsilon_{1,1}} = (\bar{k}_2 + \bar{k}_5)(\bar{k}_3 + \bar{k}_6)\left(\bar{k}_2 + \bar{k}_3 + \bar{k}_4 + 2\omega^2 m_1\right)$$

$$\bar{k}_i = k_i - \omega^2 \tfrac{1}{2} m_i \tag{40}$$

The zeros of the strain-based FRF for element 1 are given by the roots of the polynomial in the preceding equation:

$$(\bar{k}_2 + \bar{k}_5) = 0, \qquad (\bar{k}_3 + \bar{k}_6) = 0$$

$$\left(\bar{k}_2 + \bar{k}_3 + \bar{k}_4 + 2\omega^2 m_1\right) = 0 \tag{41}$$

Observe that the stiffness of element 1 is not present in the expression for $z_{\epsilon_{1,1}}$. The only presence of attributes from element 1 comes from the mass m_1. Hence, we conclude that unless the mass is changed from the reference model, the zeros of strain-based FRFs corresponding to element 1 are invariant with respect to its corresponding element stiffness. For other elements, a similar claim can be established. This illustrates the validity of the proposed damage detection criterion.

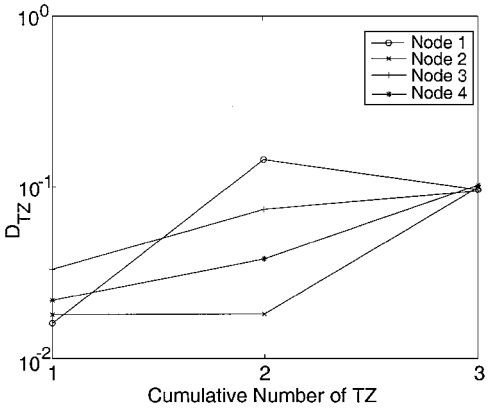

Fig. 4 Global cumulative TZ deviation.

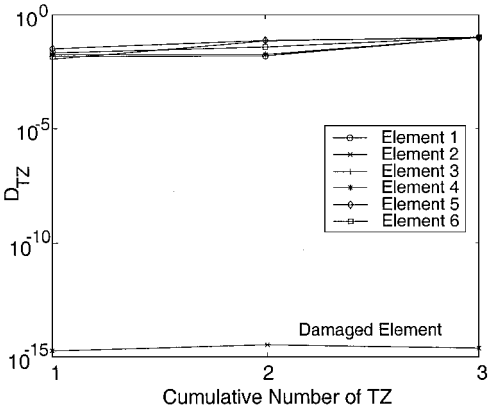

Fig. 5 Strain-based cumulative TZ deviation.

The TZ variation measure can be computed for the example if numerical values are assigned to the mass and stiffness. For the values given in Fig. 3, with damage modeled as a 50% reduction in stiffness in k_2, the plots of $\boldsymbol{D}_{\mathrm{TZ}}$ for the global and localized collocated transfer function partitions are shown in Figs. 4 and 5. Clearly, in the global case each of the TZ sets, computed for collocated transfer functions at each of the four nodes, vary with the introduction of damage. On the other hand, the strain-based TZs give a clear indication of the damaged element. The variation in the TZ set corresponding to element 2 is very small, basically to the order of the machine accuracy. This is many orders of magnitude smaller than the variation in the other TZ sets. Therefore, it can be correctly concluded that element 2 is the location of damage.

An important consideration in the identification and utilization of TZs for damage detection purposes is their behavior in the presence of damping. It is common to see damping rise by an order of magnitude with the onset of damage. Therefore, the question of how damping effects TZs must be addressed. If damping is assumed to be proportional, then $\bar{k}_i$ from Eq. (40) can be modified to

$$\bar{k}_i = k_i + j\omega\left(\tfrac{1}{2}\alpha m_i + \beta k_i\right) - \tfrac{1}{2}\omega^2 m_i \tag{42}$$

so that each of the zero values from Eq. (41) can modified accordingly. Nevertheless, the magnitude of the zeros are not affected by the presence of damping because for a parabolic equation given by

$$as^2 + bs + c = 0, \qquad s = j\omega \Rightarrow |s^2| = c/a \tag{43}$$

regardless of the magnitude of b. For nonproportional damping, as long as it can be partitioned consistently, the same conclusion holds.

Illustrative Examples

The objective of our damage detection scheme is to uniquely determine the damage location in a structure by tracking the TZs of partitions of $\mathcal{H}_\epsilon$. To illustrate the theory in the preceding sections, we present two examples. The first is a 16-element plane beam structure, for which the TZs are calculated numerically. The second is an illustration of the effects of modal truncation and residual flexibility on the TZ calculation. It is shown that the inclusion of a residual term along with the truncated set of identified modes is sufficient to determine the location of damage in this manner.

Simulated Indeterminate Beam Model

The first example presented is an indeterminate 16-element simplification of an engine mount structure, or ladder, shown in Fig. 6. Each beam element has 3 DOF per node, or 36 global DOF. The substructural model has 48 DOF, corresponding to, for each element, two bending strains, measured at the Gauss points, and one longitudinal strain, measured at the element midpoint, as is shown in Fig. 6. The case we consider here models damage as a 70% reduction in stiffness in element 10.

It is clear that more realistic problems are prohibitively large to compute or write in analytical form as was possible for the spring–mass system. In fact, whereas it is possible to calculate the global and local transfer function matrix analytically, it is virtually impossible to calculate the transmission zeros analytically. For this reason, the TZs for this example are calculated numerically in MATLAB®. This calculation is based on the state-space form of the FRF of interest using the routine by Emami-Naeini and Van Dooren[12] as implemented in MATLAB.

We say that the TZs of node n are the TZs of the MIMO transfer function matrix partition $\mathcal{H}_g(m, m)$, where the m refers to the DOF list of inputs and outputs on node n. With this in mind, the variation of TZs corresponding to global node-by-node transfer functions are presented graphically in Fig. 7, which shows the cumulative TZ variation $\boldsymbol{D}_{\mathrm{TZ}}$ computed from each partition of the global FRF

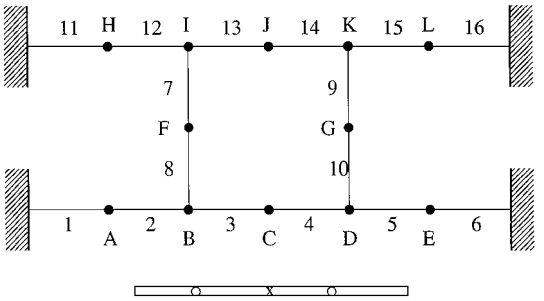

Fig. 6 Beam ladder with 16 elements and strain measurement locations.

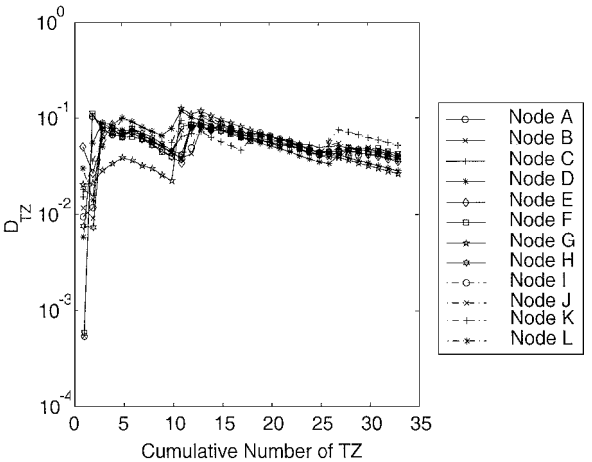

Fig. 7 Ladder global cumulative TZ deviation.

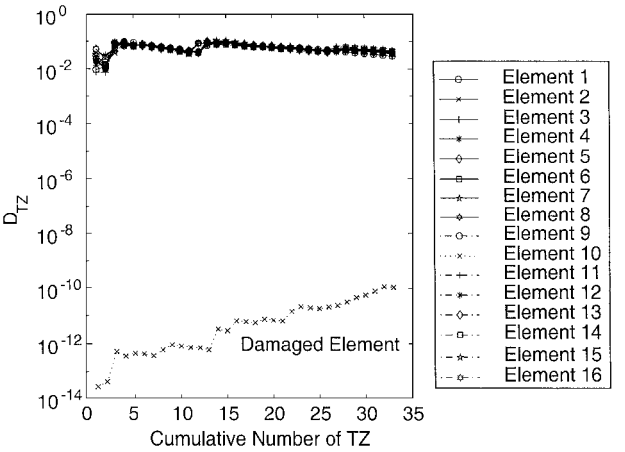

Fig. 8 Ladder strain-based cumulative TZ deviation.

corresponding to individual nodes. Note that the TZs of each global node vary with the damage, as they would vary for damage in other elements due to the flexibility coupling of the global structure. Note also that these values do not correspond to any zero values from a single matrix element $h_{gi,i}$ that are included in m.

In localized form, a plot of the strain-based $\boldsymbol{D}_{\mathrm{TZ}}$ using the analytically calculated TZs is shown in Fig. 8. Clearly, the cumulative variation in the zeros in element 10 is many orders of magnitude less than the TZ variation in the other elements. For this example, the TZ variation of element 10 is of the same order as the machine accuracy, which is as close to theoretical zero invariance as is possible to compute numerically. Recall that this is the extreme, ideal case where we have analytically computed the TZs over a frequency range that includes all of the flexible modes of the example structure. The next example investigates a more realistic scenario, where the testing frequency range is not wide enough to determine all of the system dynamics.

Limited Modal Data Case

In the preceding example, it is assumed that it is possible to measure the full modal spectrum of the structure under consideration. Clearly, this may not be realistic, as reality comes in the form of sampling, hardware and software limitations, noise, etc. Therefore, something must be done to augment the limited amount of modal information available in a realistic test. To correctly calculate the TZs, as much modal information must be included as is possible. The TZs are values of frequency at which the contribution of all of the modes sums to zero. Therefore, if some of the modes are not included, the TZ values will be incorrect. Supplementing the measured data can be done in several ways, such as model updating using an analytical reference model. However, because we wish to limit the number of modeling assumptions made, we will augment the modal data with an estimate of the residual flexibility.[13] The residual flexibility can be used as an approximation to the out-of-range high-frequency modes and, therefore, can help improve the TZ determination.

To study this case, the same engine mount structure from the earlier example was utilized. The nominal and damaged system responses were computed due to burst-random inputs at six locations for approximately 25 s at 1600 Hz. The input and output data were then resampled and filtered at 400 Hz, which should capture the 12 flexible modes below 200 Hz. These filtered inputs and outputs were then used in a system identification procedure to determine the modal frequencies, mode shapes, and the residual flexibility term. These results are then used to determine the TZs of select input/output sets of the structure.

Representative results of this exercise can be seen in Fig. 9, which shows that element 10 has the lowest cumulative error over the span of calculated TZs. In this realistic example, the difference in $\boldsymbol{D}_{\mathrm{TZ}}$ is not nearly as great as in the earlier example. In fact, in this case the difference is not even one order of magnitude. However, the trend clearly indicated in Fig. 9 is that the damaged element, element 10, has the lowest TZ variation over the range of zeros in the set.

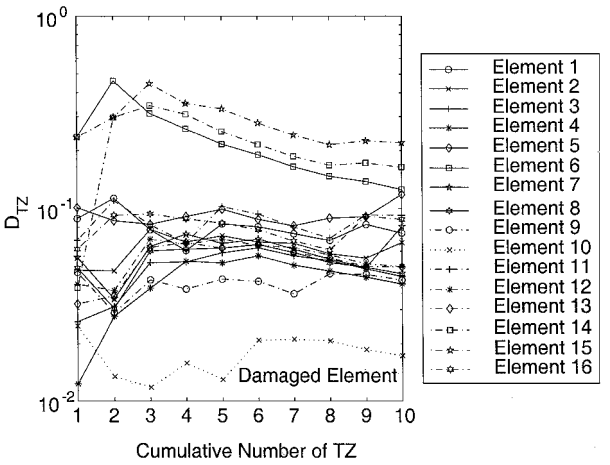

Fig. 9 Limited mode case strain-based cumulative TZ deviation.

From these data, the conclusion can be made that this proposed procedure can correctly identify the damage location, provided a sufficient amount of modal data is available. If possible, the residual flexibility term should also be determined and included in the analysis. Obviously, if there is more modal information in the residual than is identified directly, the calculated TZ values will be greatly suspect, and this procedure is likely to fail.

Conclusions

A method for structural health monitoring based on an invariance property of the TZs of substructural transfer functions has been presented. Damage in a substructure can be uniquely identified by monitoring the zeros of the corresponding localized transfer function. Damage is indicated by a change in the system response characteristics without a corresponding change in the TZs.

The keys to the present method are the decomposition of the global dynamic flexibility into a localized form and the identification and tracking of the TZs of each localized substructure. The partitioning process rewrites the system dynamics in terms of substructural variables. The TZs are utilized because of their dependence on the inputs and outputs of the corresponding transfer function.

The TZs of global transfer functions are shown to be invariant only for elements on a fixed boundary and, therefore, are not generally useful for health monitoring in this manner.

To the best of the authors' knowledge, the use of substructural TZs for health monitoring and damage detection is presented in this paper first. It is a natural extension of the flexibility partitioning procedure applied to the dynamic case, and its effects on the system poles and zeros are clear.

For this method of structural damage detection to be used in a practical manner, there are several issues that must be addressed. In particular, the application of this method to continuum structures has been addressed, although not covered in this paper. However, this still needs to be investigated in a more systematic manner. Additionally, the localized form assumes that local inputs at all DOFs are available by transforming a limited global forcing input. An investigation into the localized controllability of the structure in question is required.

Perhaps the most important issue that must be studied is identification of the TZs themselves. System realization methods that capture localized zeros accurately would render the proposed method attractive for practical applications.

Acknowledgments

The first author would like to acknowledge funding from the U.S. Air Force Palace Knight Program. The second author wishes to thank Sandia National Laboratory and Shimizu Corporation for their support in carrying out the work reported herein.

References

[1]Sun, F. P., Chaudhry, Z., Rogers, C. A., Majmundar, M., and Liang, C., "Truss Structure Integrity Identification Using PZT Sensor–Actuator," *Journal of Intelligent Material Systems and Structures*, Vol. 6, No. 1, 1995, pp. 134–139.

[2]Hickman, G. A., Gerardi, J. J., and Feng, Y., "Application of Smart Structures to Aircraft Health Monitoring," *Journal of Intelligent Material Systems and Structures*, Vol. 2, No. 3, 1991, pp. 411–430.

[3]Doebling, S. W., Farrar, C. R., Prime, M. B., and Shevitz, D. W., "Damage Identification and Health Monitoring of Structural and Mechanical Systems from Changes in Their Vibration Characteristics: A Literature Review," Los Alamos National Lab., Rept. LA-13070-MS, Los Alamos, NM, May 1996.

[4]Park, K. C., Reich, G. W., and Alvin, K. F., "Structural Damage Detection Using Localized Flexibilities," *Journal of Intelligent Material Systems and Structures*, Vol. 9, No. 11, 1998, pp. 911–919.

[5]Alvin, K. F., and Park, K. C., "A Partitioned System Identification Procedure for Substructural Flexibility Determination," AIAA Paper 96-1297, 1996.

[6]Park, K. C., and Reich, G. W., "Localized System Identification and Structural Monitoring from Vibration Test Data," AIAA Paper 97-1318, 1997.

[7]Park, K. C., and Reich, G. W., "A Theory for Strain-Based Structural System Identification," *Adaptive Structures and Technologies*, edited by N. W. Hagood and M. J. Attala, Technomic, Lancaster, PA, 1999, pp. 83–93.

[8]Afolabi, D., "An Anti-Resonance Technique for Detecting Structural Damage," *Proceedings of the 5th International Modal Analysis Conference*, Union College, Schenectady, NY, 1987, pp. 491–495.

[9]Park, K. C., and Felippa, C. A., "A Variational Framework for Solution Method Developments in Structural Mechanics," *Journal of Applied Mechanics*, Vol. 65, No. 1, 1998, pp. 242–249.

[10]Park, K. C., and Felippa, C. A., "A Variational Principle for the Formulation of Partitioned Structural Systems," *International Journal for Numerical Methods in Engineering*, Vol. 47, No. 1–3, 2000, pp. 395–418.

[11]Horn, R. A., and Johnson, C. R., *Matrix Analysis*, Cambridge Univ. Press, Cambridge, England, U.K., 1985, pp. 17–21.

[12]Emami-Naeini, A., and Van Dooren, P., "Computation of Zeros of Linear Multivariable Systems," *Automatica*, Vol. 18, No. 4, 1982, pp. 415–430.

[13]Peterson, L. D., and Alvin, K. F., "Time and Frequency Domain Procedure for Identification of Structural Dynamic Models," *Journal of Sound and Vibration*, Vol. 201, No. 1, 1997, pp. 137–144.

A. Berman
Associate Editor